Electronic Supplementary Information (ESI)

General and Facile Synthesis of Hollow Metal Oxide Nanoparticles Coupling with Graphene Nanomesh Architectures for Highly Efficient Lithium Storage

Zheye Zhang, Xin Tian, Mingli Liu, Pei Xu, Fei Xiao and Shuai Wang*

Key laboratory of Material Chemistry for Energy Conversion and Storage, Ministry of Education, School of Chemistry and Chemical Engineering, Huazhong University of Science and Technology, Wuhan, 430074, China

Corresponding author: chmsamuel@mail.hust.edu.cn (S. Wang)

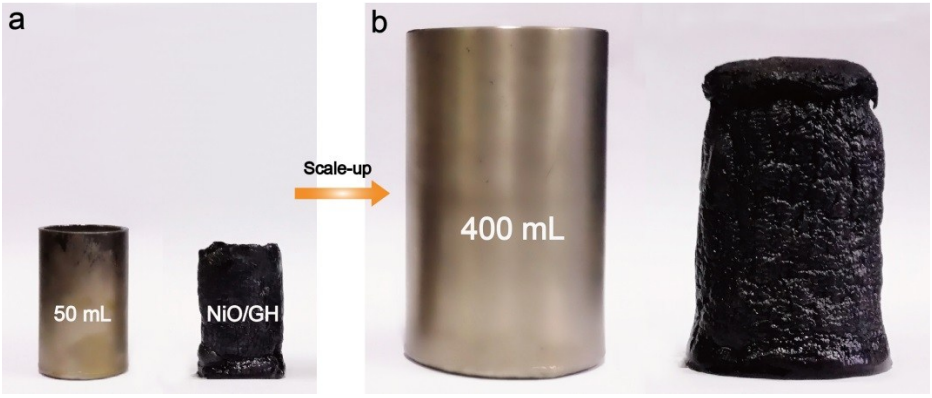

Figure S1. The photograph of a monolithic NiO/GH with (a) 50 mL Ni vessel and (b) 400 mL Ni vessel.

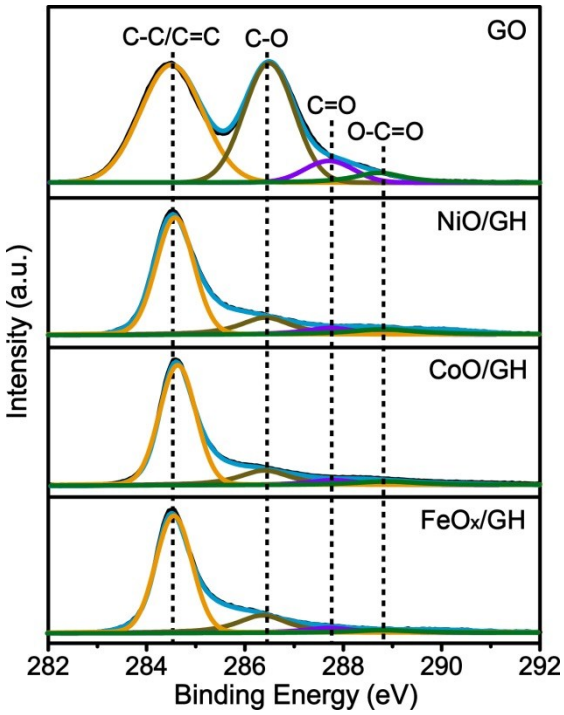

Figure S2. XPS C 1s spectra of GO, NiO/GH, CoO/GH and FeO_x/GH.

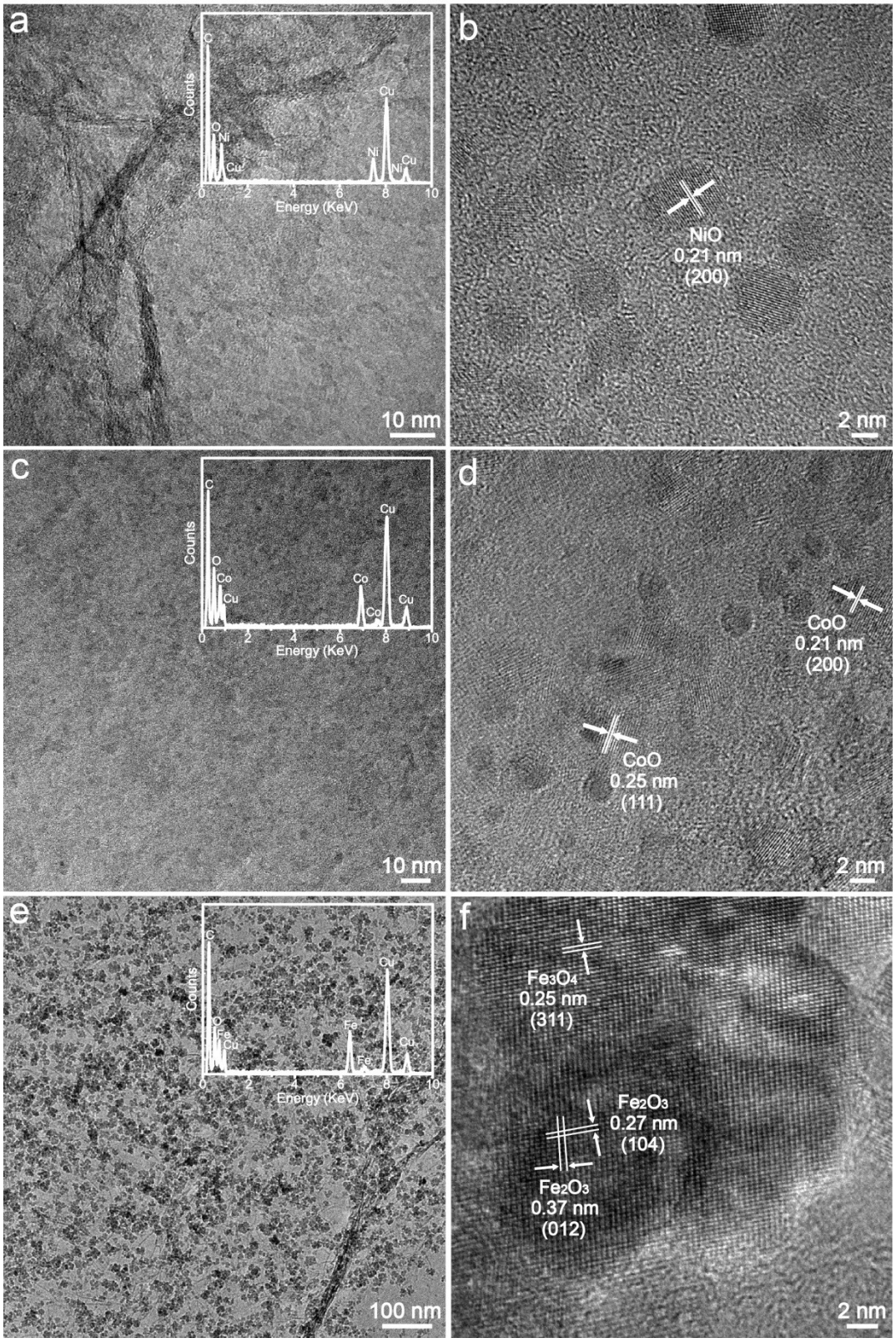

Figure S3. TEM images of (a,b) NiO/GH, (c,d) CoO/GH and (e,f) FeO_x/GH. Inset in (a), (c) and (e) are the corresponding EDX spectra.

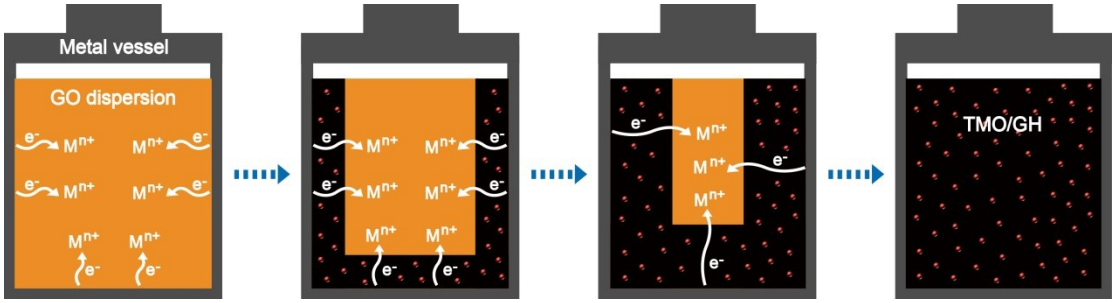

Figure S4. Schematic illustration of the formation process of TMO/GH.

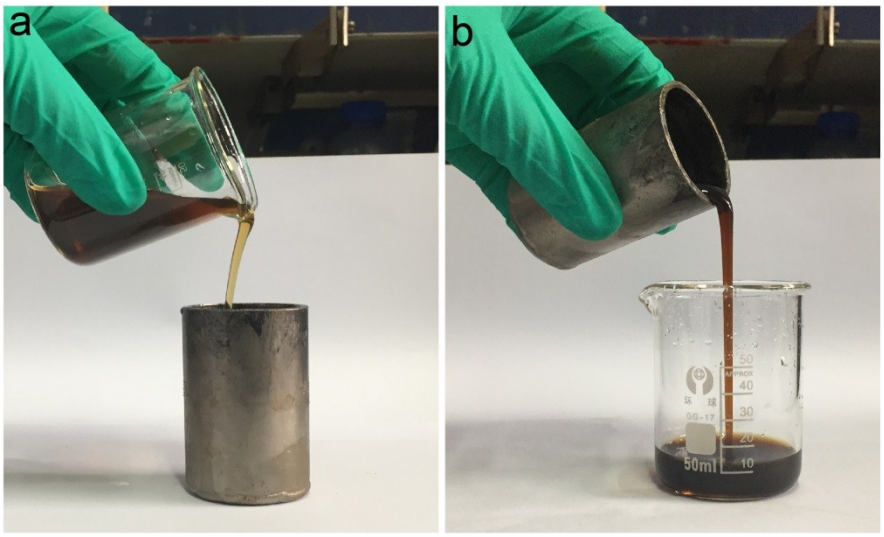

Figure S5. Room temperature reaction. (a) before and (b) after 40 h reaction. Only a dark-brown despersion can be observed after reaction.

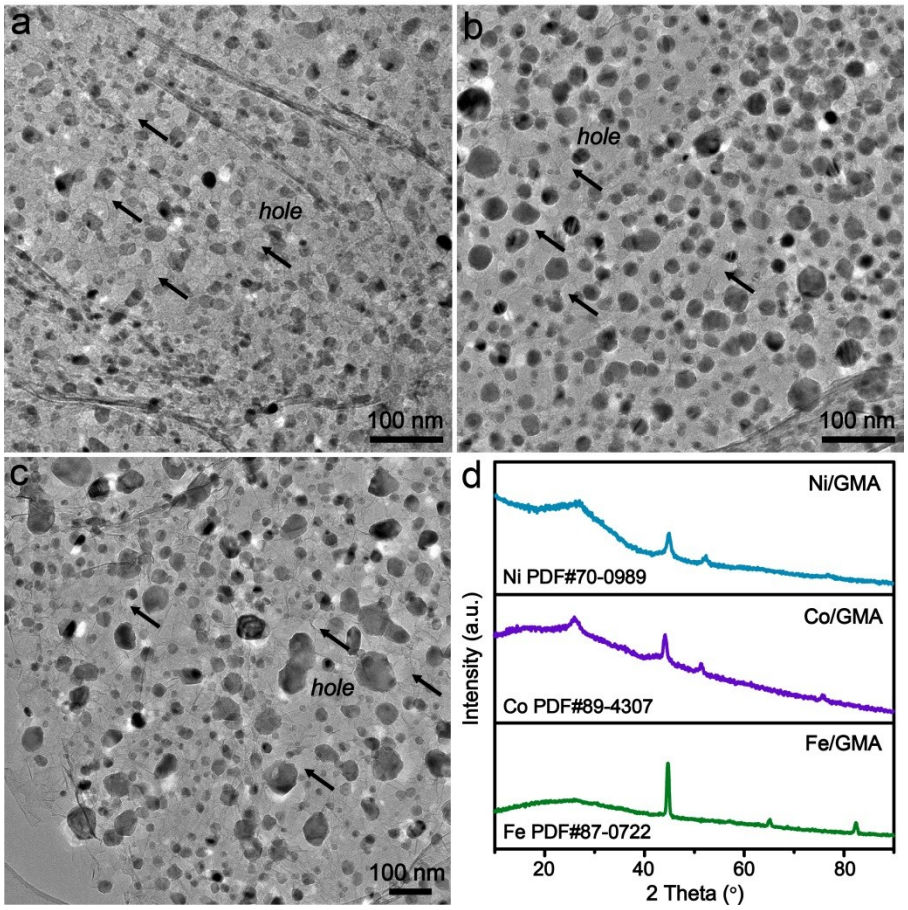

Figure S6. TEM images of (a) Ni/GMA, (b) Co/GMA and (c) Fe/GMA. (d) XRD patterns of various TM/GMAs.

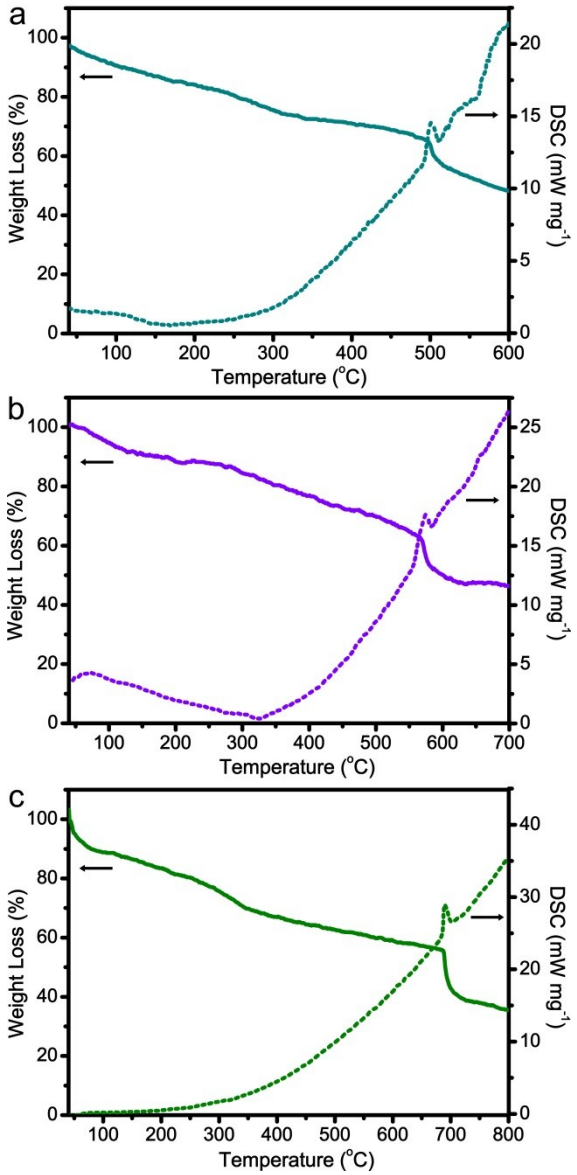

Figure S7. TGA/DSC curves of (a) NiO/GH, (b) CoO/GH and (c) FeO_x/GH.

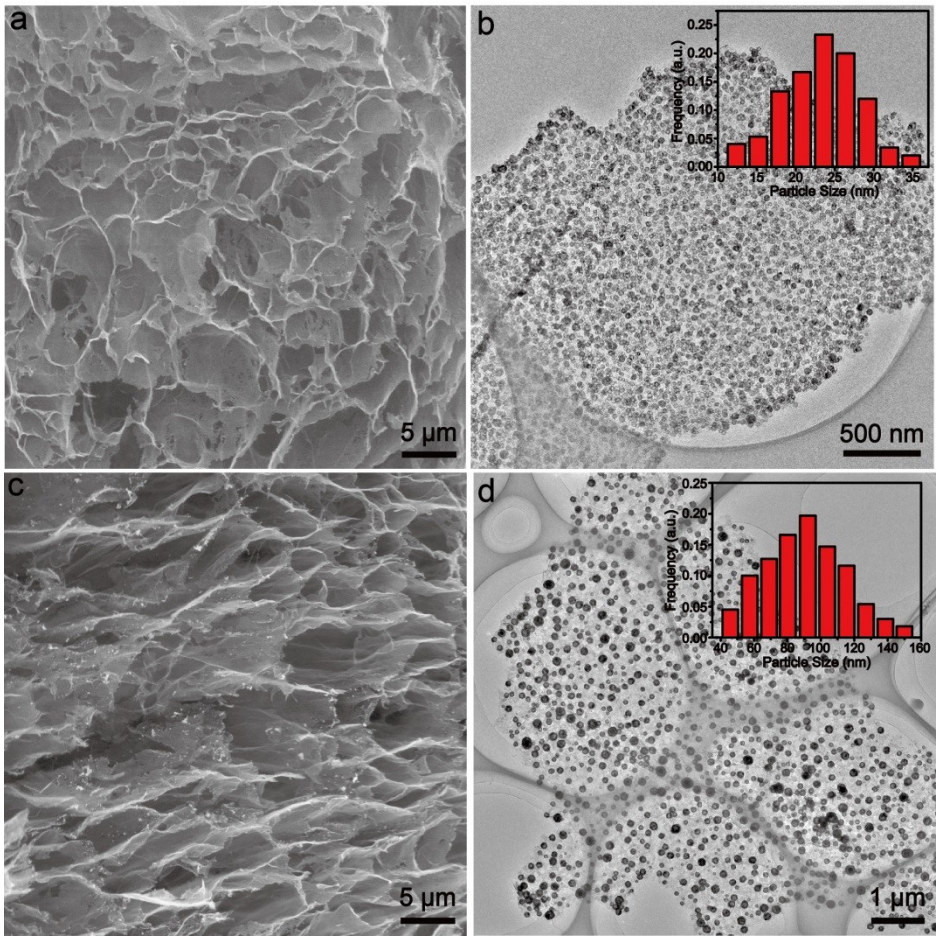

Figure S8. (a) SEM and (b) TEM images of H-Co_3O_4/GMA. (c) SEM and (d) TEM images of H-FeO_x/GMA. Inset in (b) and (d) are the corresponding particle size distribution histograms.

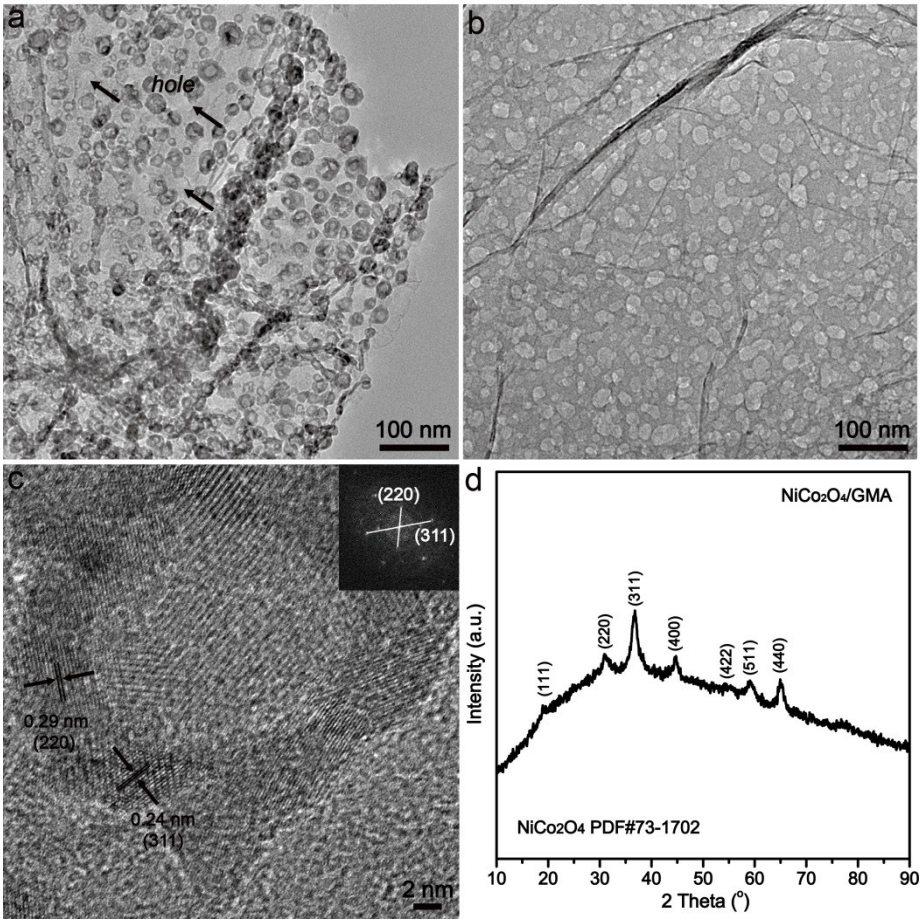

Figure S9. (a-c)TEM images of H-$NiCo_2O_4$/GMA. (d) XRD pattern of H-$NiCo_2O_4$/GMA. Inset in (c) is the corresponding FFT pattern.

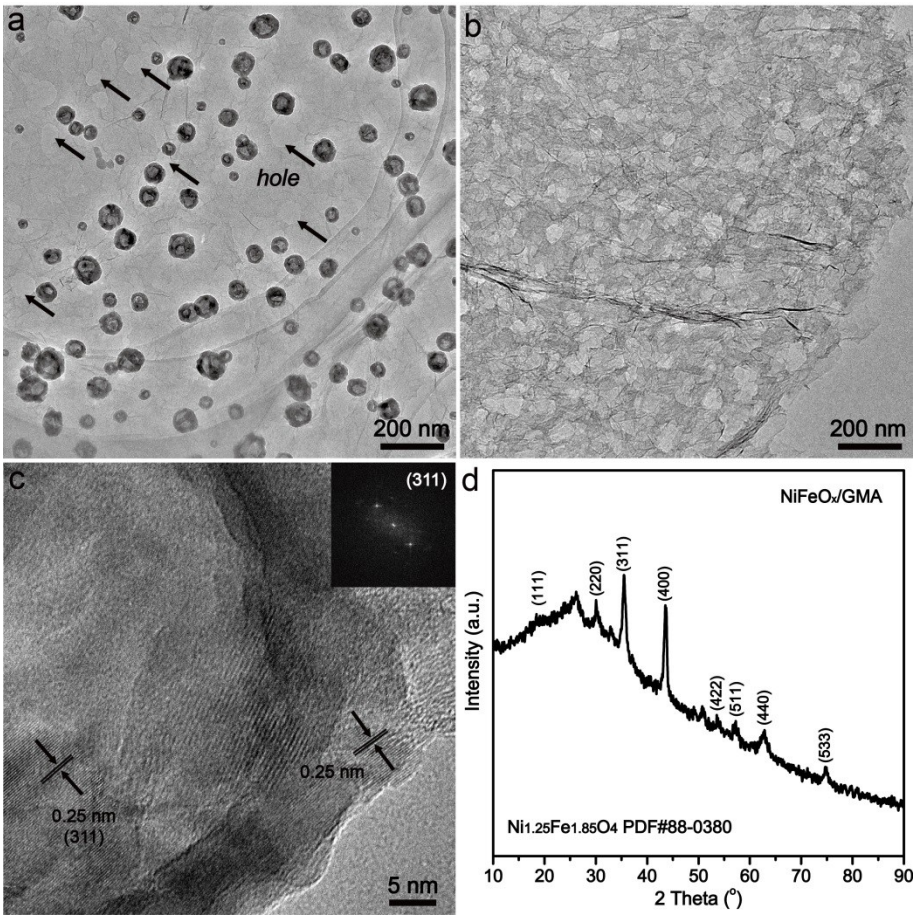

Figure S10. (a-c)TEM images of H-$NiFeO_x$/GMA. (d) XRD pattern of H-$NiFeO_x$/GMA. Inset in (c) is the corresponding FFT pattern.

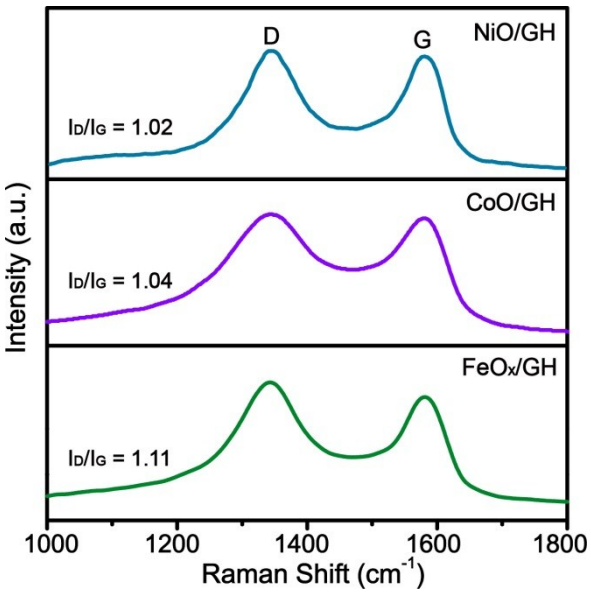

Figure S11. Raman spectra of NiO/GH, CoO/GH and FeO_x/GH.

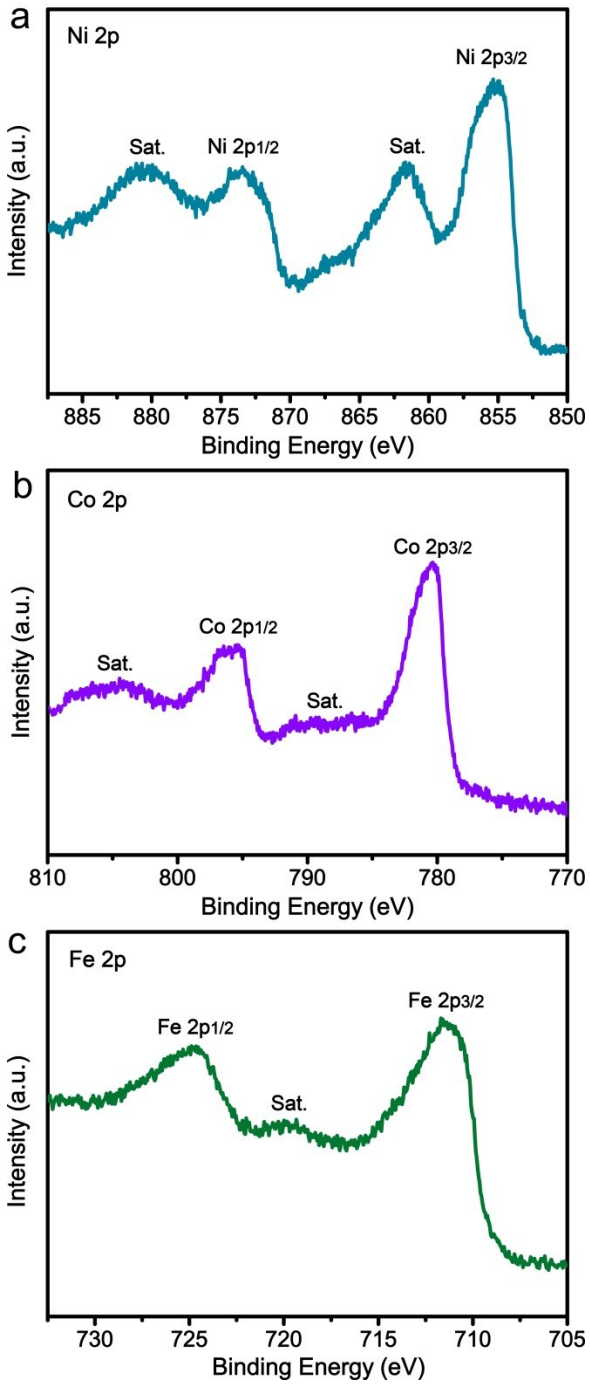

Figure S12. (a) Ni 2p XPS spectra of H-NiO/GMA. (b) Co 2p XPS spectra of H-Co_3O_4/GMA. (c) Fe 2p XPS spectra of H-FeO_x/GMA.

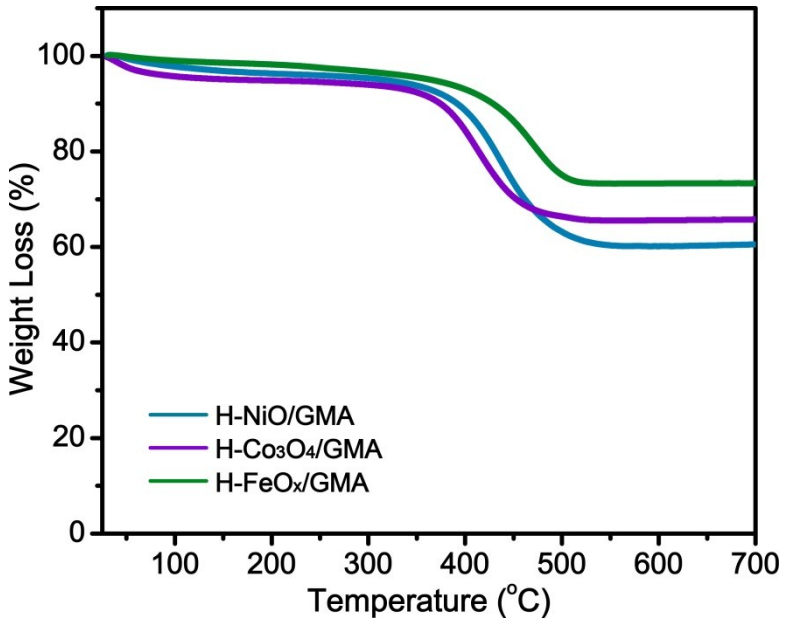

Figure S13. TGA curves of H-NiO/GMA, H-Co_3O_4/GMA and H-FeO_x/GMA in air atmosphere.

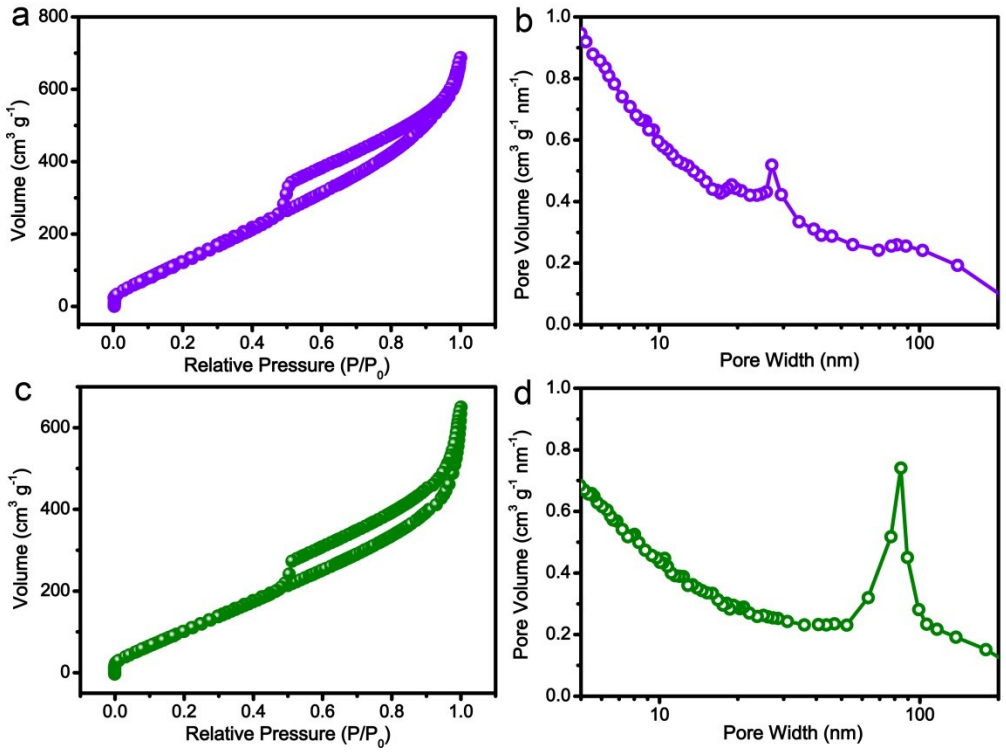

Figure S14. N_2 adsorption-desorption isotherms of (a) H-Co_3O_4/GMA and (c) H-FeO_x/GMA. Pore size distribution of (b) H-Co_3O_4/GMA and (d) H-FeO_x/GMA.

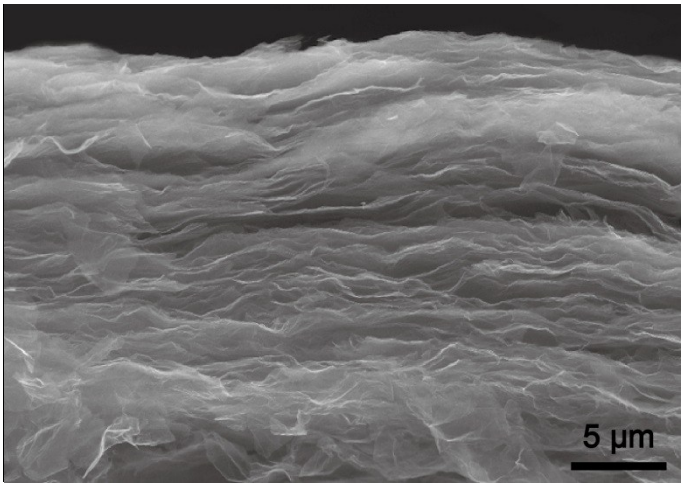

Figure S15. Cross-sectional SEM image of the compressed H-NiO/GMA.

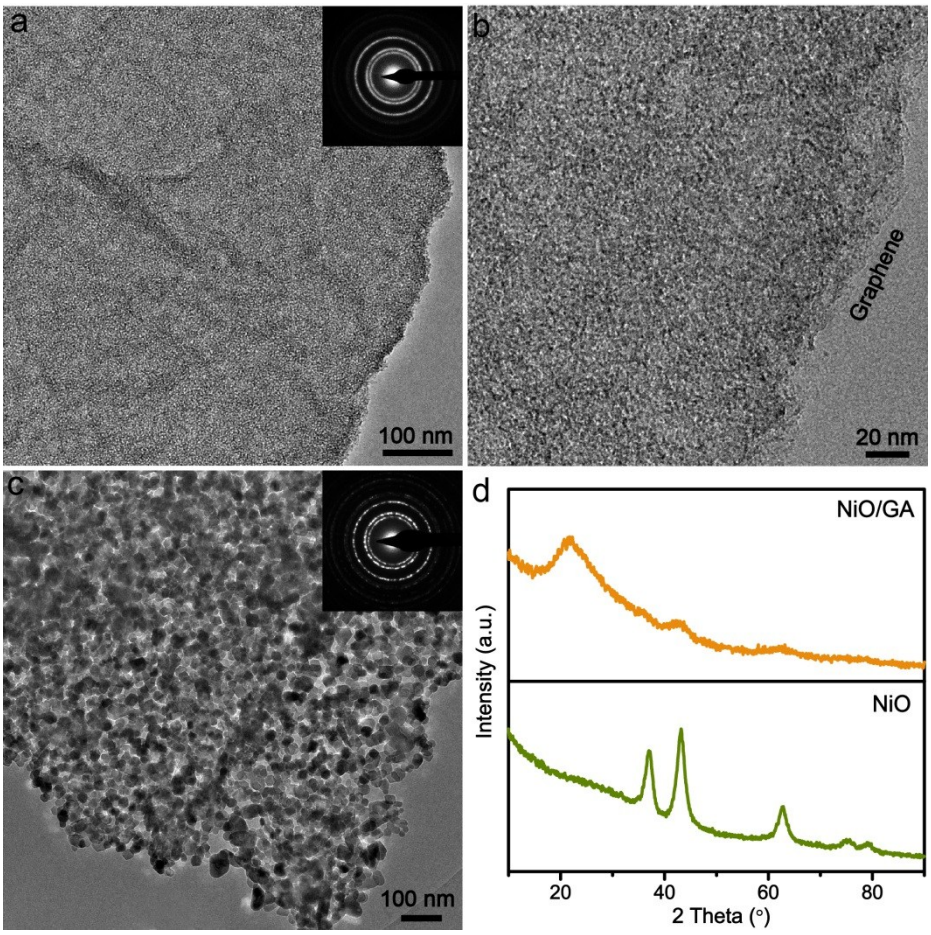

Figure S16. TEM images of (a,b) NiO/GA and (c) pure NiO. (d) XRD patterns of NiO/GA and pure NiO. Inset in (a) and (c) are the corresponding SAED patterns.

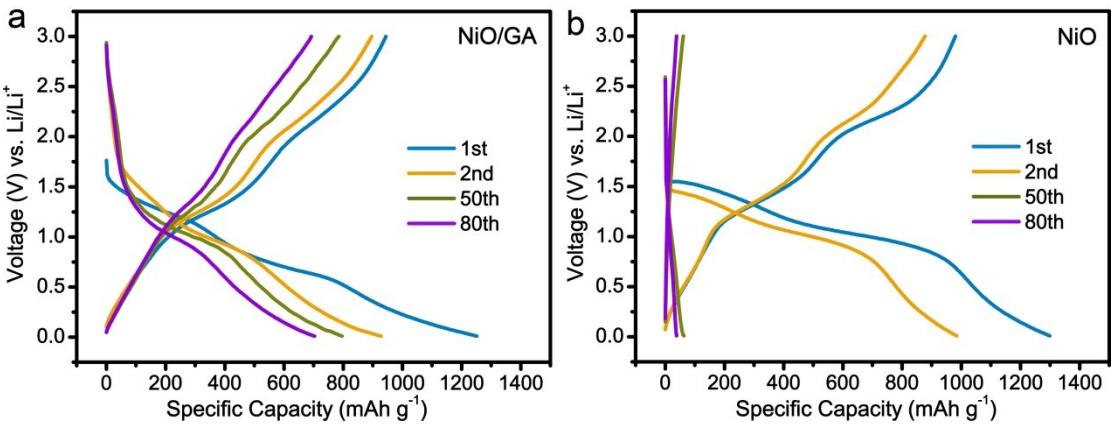

Figure S17. Discharge/charge profiles of (a) NiO/GA and (b) pure NiO electrodes at a current density of 0.2 A g^{-1}.

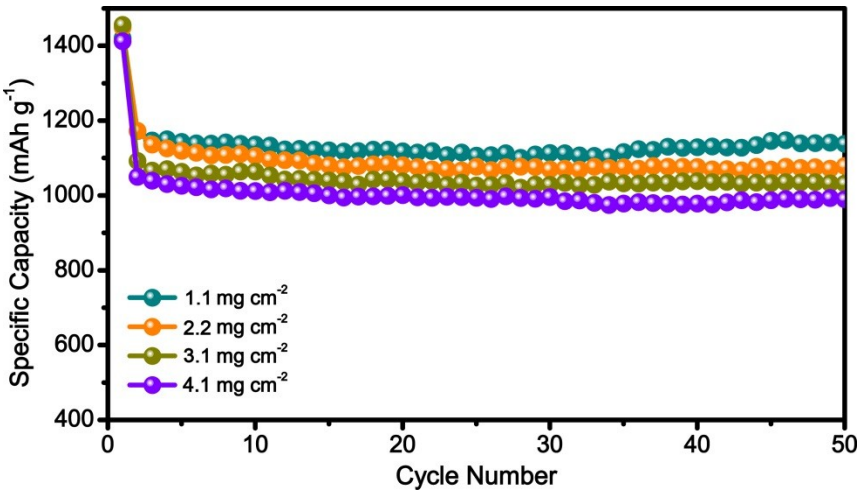

Figure S18. Cycling performance of H-NiO/GMA electrode with different loading amounts at a current density of 0.2 A g^{-1}.

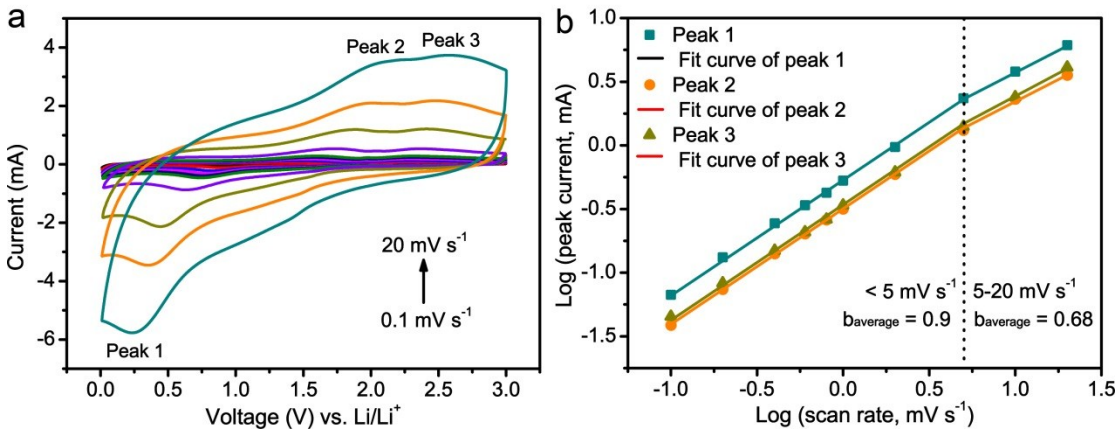

Figure S19. Kinetics analysis of the electrochemical behavior of the NiO/GA electrode. (a) CV curves at various scan rates from 0.1 to 20 mV s^{-1}. (b) b-value analysis using the relationship between the peak currents and the scan rates.

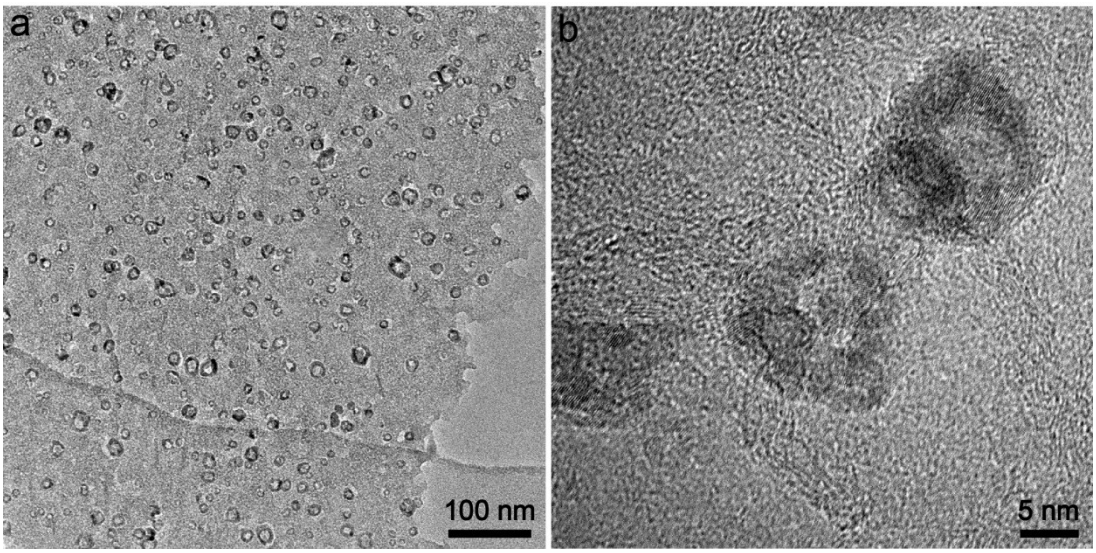

Figure S20. (a) TEM and (b) HRTEM images of H-NiO/GMA after cycling test.

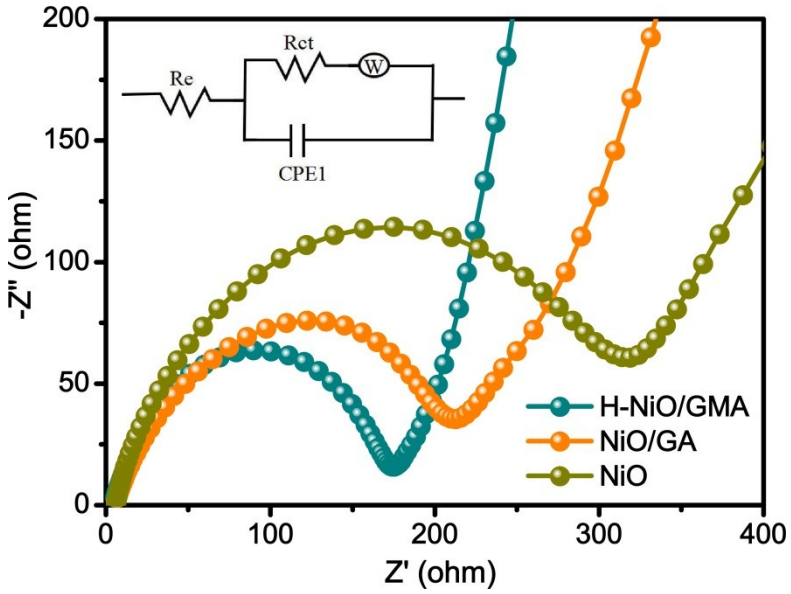

Figure S21. EIS spectra of H-NiO/GMA, NiO/GA and pure NiO electrodes. Inset is the corresponding equivalent circuit model. R_e shows the resistance of electrolyte, R_{ct} is the charge transfer resistance, CPE shows the double layer capacitance and W is the Warburg impedance.

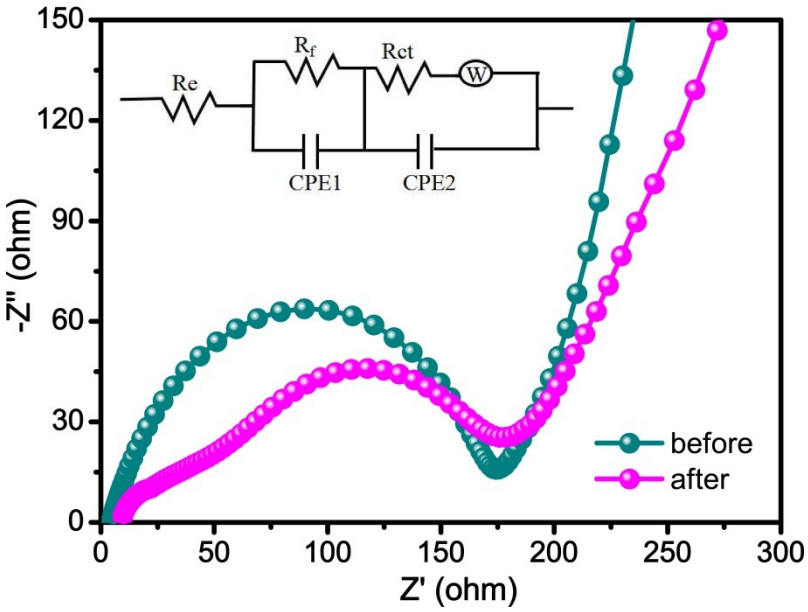

Figure S22. EIS spectra of H-NiO/GMA electrode before and after cycling. Inset is the equivalent circuit model after cycling. R_f is the resistance of SEI film.

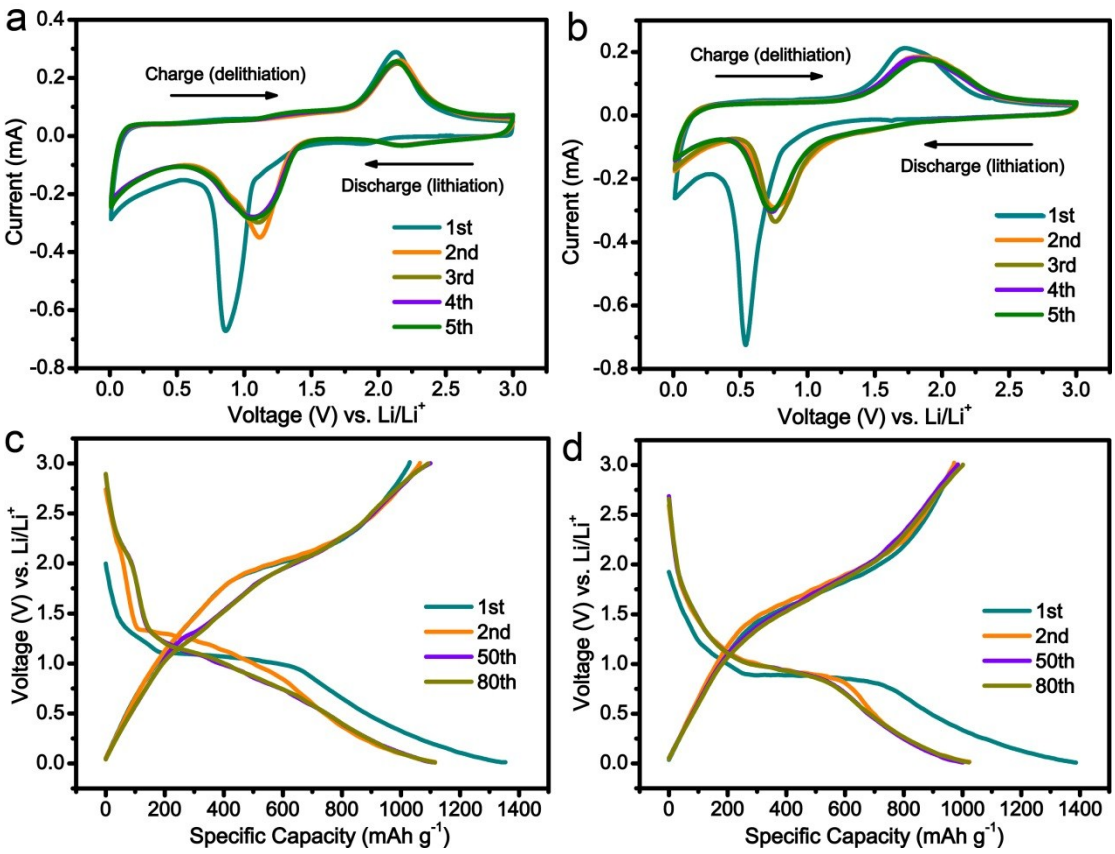

Figure S23. (a) CV curves and (c) discharge/charge profiles at 0.2 A g^{-1} of H-Co_3O_4/GMA electrode. (b) CV curves and (d) discharge/charge profiles at 0.2 A g^{-1} of H-FeO_x/GMA electrode.

Table S1. Comparison of electrochemical performance of H-NiO/GMA and recently reported typical NiO-based anode materials.

Electrodes	Mass Loading ($mg\ cm^{-2}$)	Storage Capacity ($mAh\ g^{-1}$)	Rate Capability ($mAh\ g^{-1}$)	Capacity Retention	References
NiO/graphene composites	1-2	883 (0.05 A g^{-1})	550 (2.5 A g^{-1})	90 % (50 cycles at 0.05 A g^{-1})	1
Triple-shelled NiO microfibers	0.7	920 (0.1 A g^{-1})	540 (5 A g^{-1})	87 % (200 cycles at 1 A g^{-1})	2
Mesoporous NiO microspheres	N.A.	800 (0.5 A g^{-1})	620 (1 A g^{-1})	114 % (100 cycles at 0.5 A g^{-1})	3
Yolk-shell NiO/GQDs microspheres	1.5	1182 (0.1 A g^{-1})	200 (5 A g^{-1})	121 % (250 cycles at 0.1 A g^{-1})	4
RGO/Ni foam	1.5	1200 (0.1 A g^{-1})	335 (3 A g^{-1})	74.3 % (300 cycles at 0.2 A g^{-1})	5
Diaper derived NiO/Ni composites	0.8	1075 (0.1 A g^{-1})	440 (4 A g^{-1})	97.6 % (400 cycles at 1 A g^{-1})	6
NiO nanowire foam	1.3	577 (0.14 A g^{-1})	75 (35.9 A g^{-1})	68 % (1000 cycles at 0.359 A g^{-1})	7
NiO nanosheets	1.5-1.8	892 (0.1 A g^{-1})	298 (5 A g^{-1})	78 % (150 cycles at 0.7 A g^{-1})	8
Porous NiO nanorods	N.A.	700 (0.1 A g^{-1})	150 (2 A g^{-1})	134 % (60 cycles at 0.1 A g^{-1})	9
Hollow NiO nanospheres/ N-doped graphene	1	1104 (0.08 A g^{-1})	422 (4 A g^{-1})	135 % (150 cycles at 0.08 A g^{-1})	10
NiO/graphene/carbon Fiber	0.7	834 (0.1 A g^{-1})	380 (2 A g^{-1})	94 % (350 cycles at 0.5 A g^{-1})	11
NiO hollow microspheres	0.8	766 (0.5 A g^{-1})	457 (10 A g^{-1})	76.4 % (100 cycles at 1 A g^{-1})	12
Porous NiO-wrapped graphene	N.A.	705 (0.2 A g^{-1})	403 (1.6 A g^{-1})	47 % (50 cycles at 0.2 A g^{-1})	13
Hollow NiO/C hybrid nanoparticle	N.A.	622 (0.2 A g^{-1})	500 (1 A g^{-1})	88.7 % (100 cycles at 1 A g^{-1})	14
Ni/MoO2 microflowers	1	994 (0.1 A g^{-1})	406 (5 A g^{-1})	90.7 % (100 cycles at 1 A g^{-1})	15
NiO-Co_3O_4@C nanocomposites	1	870 (0.1 A g^{-1})	315 (5 A g^{-1})	109 % (100 cycles at 0.1 A g^{-1})	16
SnO_2/NiO@Ag nanotubes	3	1150 (0.1 A g^{-1})	300 (10 A g^{-1})	99 % (500 cycles at 1 A g^{-1})	17
CuO@NiO hollow spheres	2	1061 (0.1 A g^{-1})	N.A.	124 % (200 cycles at 0.1 A g^{-1})	18
TiC/NiO core/shell	N.A.	636 (0.05 A g^{-1})	369 (3 A g^{-1})	90 % (60 cycles at 0.2 A g^{-1})	19
H-NiO/GMA	**1.1**	**1202 (0.1 A g^{-1})**	**574 (10 A g^{-1})**	**98 % (1000 cycles at 10 A g^{-1})**	**This work**

Table S2. The parameters obtained from the EIS on various electrodes.

Electrodes	R_e (Ω)	R_{ct} (Ω)	R_f (Ω)
H-NiO/GMA	4.8	168.6	-
(after 80 cycles)	8.5	156.4	31.5
NiO/GA	5.5	201.4	-
NiO	6.1	308.2	-
H-Co_3O_4/GMA	5.3	203.4	-
H-FeO_x/GMA	5.8	238.6	-

References

[1] G. M. Zhou, D. W. Wang, L. Yin, N. Li, F. Li, H. M. Cheng, ACS Nano, 2012, 6, 3214-3223.

[2] J. Sun, C. X. Lv, F. Lv, S. Chen, D. H. Li, Z. Q. Guo, W. Han, D. J. Yang, S. J.Guo, ACS Nano, 2017, 11, 6186-6193

[3] Z. Bai, Z. Ju, C. Guo, Y. T. Qian, B. Tang, S. G. Xiong, Nanoscale, 2014, 6, 3268-3273.

[4] X. J. Yin, H. Q. Chen, C. W. Zhi, W. Sun, L. P. Lv, Y. Wang, Small, 2018, e1800589.

[5] J. Yang, X. F. Li, S. Han, R. L. Huang, Q. Q. Wang, J. Qu, Z. Z. Yu, ChemElectroChem, 2017, 4, 2243-2249.

[6] H. H. Wei, Q. Zhang, Y. Wang, Y. J. Li, J. C. Fan, Q. J. Xu, Y. L. Min, Adv. Funct. Mater., 2018, 28, 1704440.

[7] C. Liu, C. L. Li, K. Ahmed, Z. Mutlu, C. S. Ozkan, M. Ozkan, Sci. Rep., 2016, 6, 29183.

[8] H. Long, T. L. Shi, H. Hu, S. L. Jiang, S. Xi, Z. Tang, Sci. Rep., 2014, 4, 7413.

[9] Q. Li, G. Huang, D. M. Yin, Y. M. Wu, L. M. Wang, Part. Part. Syst. Charact., 2016, 33, 764-770.

[10] J. Y. Chen, X. F. Wu, Y. Liu, Y. Gong, P. F. Wang, W. H. Li, S. P. Mo, Q. Q. Tan, Y. F. Chen, Applied Surface Science, 2017, 425, 461-469.

[11] Z. Q. Wang, M. Zhang, J. Zhou, ACS Appl. Mater. Interfaces, 2016, 8, 11507-11515.

[12] Y. W. Li, Y. Y. Zheng, J. H. Yao, J. R. Xiao, J. W. Yang, S. H. Xiao, RSC Adv., 2017, 7, 31287-31297.

[13] D. Xie, Q. M. Su, W. W. Yuan, Z. M. Dong, J. Zhang, G. H. Du, J. Phys. Chem. C, 2013,117, 24121-24128.

[14] H. Guo, Y. P. Wang, W. Wang, L. X. Liu, Y. Y. Guo, X. J. Yang, S. X. Wang, Part. Part. Syst. Charact., 2014,31,374-381.

[15] C. L. Wang, L. S. Sun, X. X. Wang, Y. Cheng, D. M. Yin, D. X. Yuan, Q. Li, L.

M. Wang, ChemElectroChem, 2017, 4, 2915-2920.

[16] G. Huang, D. M. Yin, F. F. Zhang,Q. Li, L. M. Wang, Inorg. Chem., 2017, 56, 9794-9801.

[17] C. Kim, J. W. Jung, K. R. Yoon, D. Y. Youn, S. Park, I. D. Kim, ACS Nano, 2016,10, 11317-11326.

[18] W. X. Guo, W. W. Sun, Y. Wang, ACS Nano, 2015, 9, 11462-11471 .

[19] H. Huang, T. Feng, Y. P. Gan, M. Y. Fang, Y. Xia, C. Liang, X. Y. Tao, W. K. Zhang, ACS Appl. Mater. Interfaces, 2015, 7, 11842-11848.